Bralower, T.J., Premoli Silva, I., and Malone, M.J. (Eds.)
Proceedings of the Ocean Drilling Program, Scientific Results Volume 198

9. An Early Late Paleocene Event on Shatsky Rise, Northwest Pacific Ocean (ODP Leg 198): Evidence from Planktonic Foraminiferal Assemblages[1]

Maria Rose Petrizzo[2]

ABSTRACT

A pulse of intense carbonate dissolution occurred during the early late Paleocene at 58.4 Ma. A prominent 5- to 25-cm-thick dark brown clay-rich calcareous nannofossil ooze was found on Shatsky Rise at Sites 1209, 1210, 1211, and 1212 during Ocean Drilling Program Leg 198. The layer corresponds to the lower part of planktonic foraminiferal Zone P4 and coincides with the evolutionary first occurrence of the nannolith *Heliolithus kleinpellii,* an important component of late Paleocene assemblages and a marker for the base of Zone CP5. The clay-rich layer contains common crystals of phillipsite, fish teeth, and phosphatic micronodules and corresponds to a prominent peak in magnetic susceptibility that probably reflects these high amounts of detrital and authigenic materials. Detailed quantitative analysis of planktonic foraminiferal assemblages across the clay-rich nannofossil ooze layer shows that fundamental changes in faunal composition occurred before, during, and after deposition of the clay-rich ooze. Planktonic foraminifers in the clay-rich layer are characterized by a low-diversity, largely dissolved assemblage dominated by representatives of the genus *Igorina* (mainly *Igorina tadjikistanensis* and *Igorina pusilla*). Conversely, *Igorina albeari,* morozovellids, acarininids, globanomalinids, subbotinids, and chiloguembelinids are common below the clay-rich layer, almost disappear within it, and reappear in low abundances above the clay-rich

[1]Petrizzo, M.R., 2005. An early late Paleocene event on Shatsky Rise, northwest Pacific Ocean (ODP Leg 198): evidence from planktonic foraminiferal assemblages. *In* Bralower, T.J., Premoli Silva, I., and Malone, M.J. (Eds.), *Proc. ODP, Sci. Results,* 198, 1–29 [Online]. Available from World Wide Web: <http://www-odp.tamu.edu/publications/198_SR/VOLUME/CHAPTERS/102.PDF>. [Cited YYYY-MM-DD]
[2]Dipartimento di Scienze della Terra "Ardito Desio," Università degli Studi di Milano, via Mangiagalli 34, 20133 Milan, Italy. **mrose.petrizzo@unimi.it**

Initial receipt: 5 March 2004
Acceptance: 10 September 2004
Web publication: 1 February 2005
Ms 198SR-102

layer. These changes in faunal compositions are likely a response to a change in carbonate saturation that caused increased dissolution on the seafloor owing to the shoaling of the lysocline and the carbonate compensation depth.

INTRODUCTION

The primary objective of Ocean Drilling Program (ODP) Leg 198 was to obtain high-quality and high-resolution records of the Cretaceous and Paleogene greenhouse climates. A key aspect during the cruise was locating sites along depth and latitudinal transects to provide additional dimensions to reconstruct the paleoenvironment through time. Sites 1209–1214 were drilled on the Southern High of Shatsky Rise in a 500-m range of water depths (2387–2907 m) (Fig. **F1**). A prominent 5- to 25-cm-thick clay-rich calcareous nannofossil ooze layer was found at all of these sites in early late Paleocene sediments (Bralower et al., 2002; Bralower, Premoli Silva, Malone, et al., 2002). An age of ~58.4 Ma (timescale of Berggren et al., 1995) was assigned to this layer based on the first occurrence (FO) of the nannofossil *Heliolithus kleinpellii,* a marker for the base of nannofossil Zone CP5, which lies a few centimeters below the clay-rich layer (Bralower et al., 2002; Bralower, Premoli Silva, Malone, et al., 2002). This age is in agreement with the planktonic foraminiferal zonation, which belongs to the P4 *Globanomalina pseudomenardii* planktonic foraminiferal Zone (Bralower et al., 2002; Bralower, Premoli Silva, Malone, et al., 2002).

Detailed analysis was performed on samples from selected Leg 198 holes (1209A, 1210A, 1211B, and 1212B; water depths = 2387, 2573, 2907, and 2681 m, respectively) (Table **T1**). The clay-rich ooze shows changes in thickness and color. In Holes 1209A, 1210A, and 1211B, the clay-rich layer is located between 124.80 and 211.70 meters below seafloor (mbsf) and is characterized by a dark brown color. In Hole 1212B, the clay-rich layer is located at 88.30 mbsf and the sediments are considerably lighter in color (tan to light brown) than in Holes 1209A, 1210A, and 1211B. The thickness of the clay-rich layer decreases with increasing water depth; it is 23 cm thick in Hole 1209A compared to 11 cm thick in Hole 1211B (Table **T1**).

The clay-rich layer contains common crystals of phillipsite, fish teeth, and phosphatic micronodules and corresponds to a prominent peak in magnetic susceptibility, which probably reflects the higher amount of terrigenous material as Fe-Mn coating of grains (Bralower et al., 2002; Bralower, Premoli Silva, Malone, et al., 2002). There is a direct relationship between magnetic susceptibility and the amount of phillipsite; phillipsite can be found throughout the interval characterized by high magnetic susceptibility values. The top of the event is marked by the disappearance of phillipsite and a corresponding decrease in magnetic susceptibility (Fig. **F2**). The aim of this paper is to document changes in the planktonic foraminiferal assemblages associated with the clay-rich layer interval and to determine the oceanographic conditions that gave rise to this early late Paleocene event.

METHODS

Detailed planktonic foraminiferal analysis was performed on one selected hole for each site (Holes 1209A, 1210A, 1211B, and 1212B). A

F1. Paleogeographic reconstruction of Shatsky Rise, p. 12.

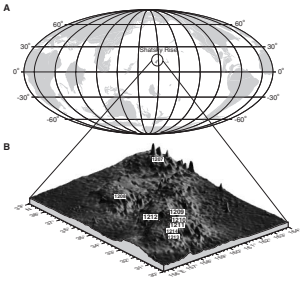

T1. Studied intervals from Leg 198 holes, p. 19.

F2. Species number and magnetic susceptibility, p. 13.

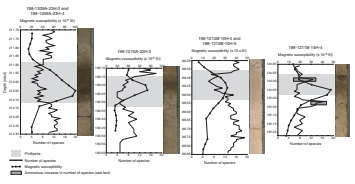

continuous U-channel taken from across the stratigraphic interval and yielding the clay-rich layer was cut into 1-cm³ samples. The high-resolution centimeter-scale sampling was extended a few centimeters below and above the clay-rich layer. A total of 185 samples were analyzed for planktonic foraminifers. Samples of ~1 cm³ were soaked in water and washed through a 38-µm sieve. The number of specimens of each species was counted in each sample in the >38-µm size fraction. Where residues were small, counts of all specimens were performed; in very small residues, <100 specimens could be counted (see Tables **T2, T3, T4, T5**). Large residues were split and an aliquot was spread over a gridded picking tray so that ~300 specimens were counted on randomly chosen grid squares. Quantitative analysis was plotted as percentages.

Planktonic Foraminiferal Assemblages

The planktonic foraminiferal assemblages in the studied stratigraphic interval are assigned to the *G. pseudomenardii* (Pl. **P1**) total range Zone P4 based on the occurrence of the nominate taxon and of *Acarinina subsphaerica*. In addition, as the FO of the nannofossil *H. kleinpellii* (marker for the base of Zone CP5) lies (T.J. Bralower, pers. comm., 2002) between the FO of *G. pseudomenardii* and the last occurrence (LO) of *Morozovella conicotruncata,* the assemblages are attributed to Subzones P4a–P4b of Berggren et al. (1995).

The assemblages throughout the studied sections are characterized by low diversity (Fig. **F2**), and they are composed mainly of three species belonging to the genus *Igorina* (*Igorina tadjikistanensis, Igorina pusilla,* and *Igorina albeari*) and two morphotypes (*I. pusilla* "high trochospire" and *I. albeari* "chubby") (see the **"Appendix,"** p. 10). Morozovellids are less abundant than igorinids in all samples (average = 20%–30%; Fig. **F3**). The acarininids are rare (Fig. **F3**) and mainly represented by *Acarinina subsphaerica* and very rare *Acarinina nitida* and *Acarinina mckannai.* Subbotinids compose <30% of the assemblage in all samples (Fig. **F4**). The smaller size fraction (<150 µm) contains rare globanomalinids and chiloguembelinids (Fig. **F4**).

High-resolution quantitative analysis of the planktonic foraminiferal assemblages indicates that fundamental changes in faunal composition occurred before, during, and after deposition of the clay-rich ooze. Changes in diversity, in state of preservation, and in the relative abundance of species can be observed in all the holes and are discussed below in stratigraphic order (from older to younger). Three intervals were identified: interval 1, interval 2, and interval 3, below, within, and above the clay-rich layer, respectively.

Interval 1—below the Clay-Rich Layer

Species richness ranges from 5 species in Hole 1210A to 19 species in Hole 1212B (Fig. **F2**). In Hole 1211B (the deeper site), an anomalously positive peak in species richness occurs 4 cm below the clay-rich layer (Samples 198-1211B-14H-4, 40–41 cm, to 14H-4, 42–43 cm; 125.00–125.02 mbsf) (Fig. **F2**). From 125.00 to 125.02 mbsf, igorinids are absent and the assemblage is composed of common *M. conicotruncata, Morozovella angulata, Morozovella acutispira,* and few *G. pseudomenardii,* which indicate correlation to Zone P4. Common representatives of the older Zone P3 (*Praemurica praecursoria, Praemurica uncinata, Morozovella praeangulata,* and *Globanomalina ehrenbergi*) are also present and clearly indicate significant reworking. Evidence of reworking was also observed

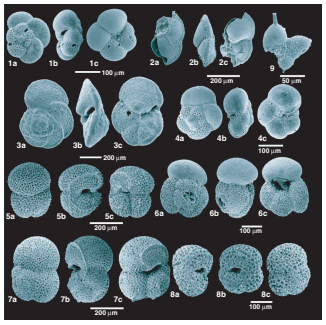

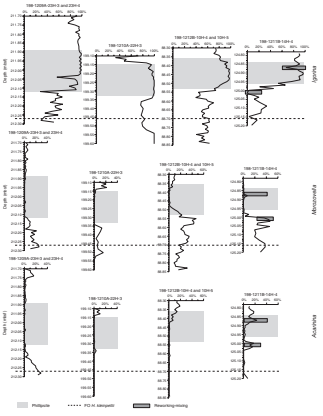

in few samples from Holes 1209A and 1212B, as revealed by the presence of sporadic small-sized taxa of Cretaceous age (*Hedbergella, Globigerinelloides* [Pl. **P2**], and *Schackoina*). Preservation ranges from moderate to poor, and common to abundant keel and wall fragments of morozovellids are present throughout (see Pl. **P3**). The very low number (<100) of total specimens counted in some samples in Holes 1212B and 1211B (see Tables **T4, T5**) is related to the very small size of the residues.

I. albeari is the most abundant species in this interval, dominating the total assemblages with an average abundance of 50% (Fig. **F5**). *I. pusilla* and *I. albeari* "chubby" are second in abundance and together constitute 40% of the assemblages (Fig. **F6**). *I. albeari* "chubby" is also characterized by marked fluctuations in abundance, especially at the shallow-water Hole 1209A. *I. tadjikistanensis* occurs in low abundance and does not exceed 20% of the total igorinids (Fig. **F5**). *I. pusilla* "high trochospire" is rare (<10% of the assemblages) except in Hole 1210A, where its abundance reaches 20% (Fig. **F6**). Morozovellids are moderately abundant in Hole 1209A (~20% of the total specimens), whereas they are more common in Hole 1212B (40% of the total specimens). The acarininids, mainly represented by *A. subsphaerica,* show a marked decrease from the base to the top of this interval in Hole 1209A and are very rare in or often absent from the other holes (Fig. **F3**). The genera *Globanomalina, Subbotina,* and *Chiloguembelina* occur in all samples, but combined they do not exceed 30% of the total assemblages. An exception is the genus *Globanomalina,* which reaches 40% and 60% of the total specimens in the deeper-water sections, Holes 1212B and 1211B, respectively (Fig. **F4**).

Interval 2—within the Clay-Rich Layer

The assemblages are characterized by very low diversity; species richness ranges from 4 species to 10 species (Fig. **F2**). An anomalous increase in the number of species occurs within the clay-rich layer in Hole 1211B (Samples 198-1211B-14H-4, 26–27 cm, to 14H-4, 28–29 cm; 124.86–124.88 mbsf). The assemblage from 124.86 to 124.88 mbsf is characterized by common *I. albeari,* morozovellids, and acarininids. Although the assemblage belongs to Subzone P4a, its composition is different from the surrounding samples that contain common crystals of phillipsite and it resembles the assemblages above the clay-rich layer. Such evidence of local mixing is probably due to drilling disturbance, as is also suggested by the lighter color of the sediment (see Fig. **F2**). The samples characterized by common to abundant phillipsite contain poorly preserved and few (<300 total specimens in the total residue) planktonic foraminifers (Pl. **P3;** Tables **T2, T3, T4, T5**).

The number of *I. tadjikistanensis, I. pusilla,* and *I. albeari* "chubby" specimens increases in interval 2 with respect to interval 1 and dominates the assemblages (average abundance = 90%–95% of the total assemblages). *I. pusilla* "high trochospire" progressively increases in abundance from the base to the top of this interval in Holes 1209A, 1212B, and 1211B, whereas it decreases uphole in Hole 1210A. *I. albeari* is absent or very rare (<3% of the assemblages) in all of the studied sections (Fig. **F5**). Morozovellids are generally absent or very rare (<1% of the assemblages) except in Hole 1212B, where the decrease in the number of morozovellid specimens is less abrupt than in the other holes and ranges from 20% to 1% in the lowermost 5 cm of the clay-rich layer. Acarininids are absent or rare (<5% of the assemblages) in Holes 1209A and 1210A, whereas a progressive increase in the number of acarininids

F4. *Globanomalina, Chiloguembelina,* and *Subbotina* relative abundances, p. 15.

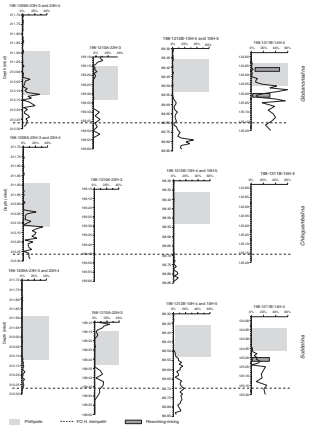

P2. *Morozovella* and *Globigerinelloides* specimens, p. 27.

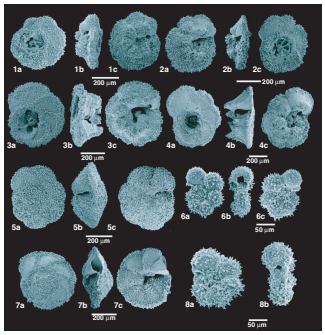

P3. Washed residues selected from three intervals, p. 28.

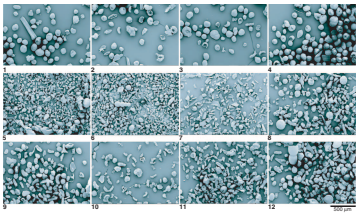

from the base (1%) to the top (average = 15%) of the interval is observed in Holes 1212B and 1211B (Fig. F3). The number of globanomalinids decreases from the base (40% of the assemblages) to the top (<1%) of the interval in Holes 1212B and 1211B; globanomalinids are almost absent in the other holes. Chiloguembelinids are generally absent or very rare (<4% of the assemblages) except for an anomalous peak (13%) in Hole 1209A that is coincident with the sudden decrease in igorinid abundance. Subbotinids are generally rare or absent (Fig. F4).

Interval 3—above the Clay-Rich Layer

The number of species ranges from 8 species in Hole 1210A to 18 species in Hole 1212B (Fig. F2). Preservation ranges from poor to moderate, and few to common fragments of morozovellids still are present (Pl. P3). There are slightly fewer *I. tadjikistanensis, I. pusilla,* and *I. albeari* "chubby" in interval 3, although they continue to dominate the assemblages in each hole (average = 70%) (Figs. F5, F6). A marked decrease in the abundance of igorinids is observed in Hole 1210A, including an abrupt decrease of *I. tadjikistanensis* (to 2%–3% of the assemblages), whereas *I. albeari* increases markedly (as much as 40% of the assemblages). In the other holes, the abundance of *I. albeari* progressively increases but never exceeds 30% of the total assemblages. The abundance of morozovellids and acarininids is low (<20%) (Fig. F3). Globanomalinids are absent except in Hole 1210A, where they reach 20% of the assemblages. Chiloguembelinids are a minor component of the assemblages in this interval (Fig. F4).

REMARKS

The faunal variations described above are associated with differences in preservation that range from moderate in the intervals of high diversity (above and below the clay-rich layer) to poor in the interval of low species richness (within the clay-rich layer) (Fig. F2; Pl. P3). Such overall moderate to poor preservation is an effect of differential dissolution, which is more significant within the clay-rich layer. In general, planktonic foraminiferal species vary in their susceptibility to dissolution and in the structural changes that occur during dissolution. In the studied samples, common to abundant keel and wall fragments of morozovellids are present throughout. Igorinids (except for *I. albeari*) are characterized by heavy overgrowth (shell thickening) (see Pl. P4) and exhibit a calcite crust that covers the outside of the test, inhibiting dissolution. The abundance of igorinids, especially in the clay-rich layer, is emphasized by the rarity and/or absence of the other genera and by the low number of total specimens (often <300 specimens) in the residues that contain abundant crystals of phillipsite. Among the igorinids, *I. tadjikistanensis, I. pusilla, I. albeari* "chubby", and *I. pusilla* "high trochospire" are the most dissolution-resistant taxa and are the only species recorded in the clay-rich layer. Conversely, *I. albeari,* morozovellids, acarininids, globanomalinids, subbotinids, and chiloguembelinids are quite common below the clay-rich layer, they almost disappear within it, and they reappear in low abundance above the clay-rich layer and are interpreted as more dissolution-susceptible taxa.

The assemblages below the clay-rich layer are different in composition: acarininids, igorinids, and *I. albeari* dominate in the shallower

F5. *I. tadjikistanensis, I. albeari,* and *I. pusilla* relative abundances, p. 16.

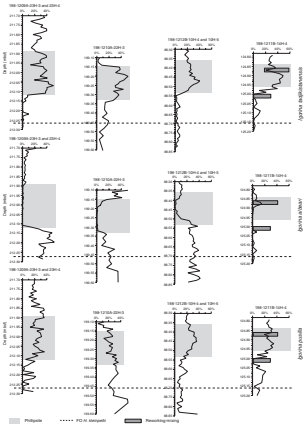

F6. *I. pusilla* "high trochospire" and *I. albeari* "chubby" relative abundances, p. 17.

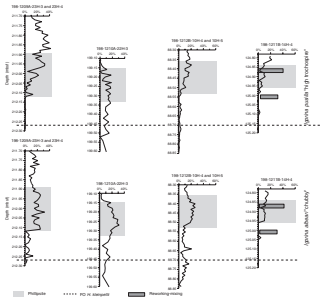

P4. *Igorina* specimens and morphotypes, p. 29.

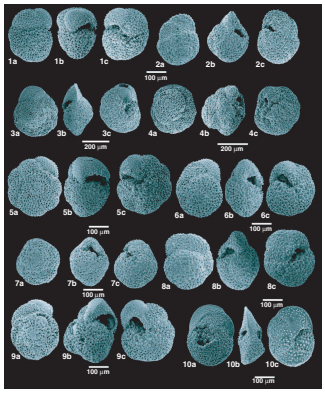

holes (1209A and 1210A), whereas morozovellids, subbotinids, and globanomalinids are more abundant in the deeper holes (1212B and 1211B). Such variations might be related to the different water depths at the studied sites (Table T1), the different susceptibilities to dissolution of the planktonic foraminiferal species, and the variations in the degree of calcite dissolution in the water column.

DISCUSSION AND CONCLUSIONS

The early late Paleocene event at Shatsky Rise can be identified by comparing the changes in faunal compositions observed in the planktonic foraminiferal assemblages between holes, the magnetic susceptibility, and the presence of phillipsite. A sequence of steps can be recognized, in stratigraphic order from older to younger (Fig. F7):

1. The FO of the nannofossil *H. kleinpellii;*
2. An increase in the abundance of *H. kleinpellii* (T.J. Bralower, pers. comm., 2003);
3. A sharp increase in magnetic susceptibility;
4. Deposition of phillipsite, an abrupt increase in the abundance of *I. tadjikistanensis,* and a sudden decrease of *I. albeari;*
5. Maximum abundances of phillipsite in the interval containing high magnetic susceptibility values (in this interval, *I. albeari* is absent or rare [<2% of the assemblages], whereas *I. tadjikistanensis* is the most abundant species); and
6. The disappearance of phillipsite and decreasing magnetic susceptibility, an increase in the abundance of *I. albeari,* and a decrease in the number of specimens of *I. tadjikistanensis*.

The onset of the event seems to occur at the same time in sections from all holes, although the signal is stronger in the shallower holes (1209A and 1210A), where the magnetic susceptibility values are higher (80–100 × 10^{-5} SI) and the clay-rich layer is thicker (Fig. F7; Table T1). In these shallower holes, the beginning of the sharp increase in magnetic susceptibility values, the deposition of phillipsite, and the change in faunal composition are almost coincident.

Conversely, in the deeper holes (1212B and 1211B) the sequence of temporal steps is less clear, as the beginning of the sharp increase in magnetic susceptibility values seems to precede the deposition of phillipsite. In Hole 1211B, the delay in the deposition of phillipsite is the result of mixing, as shown by the planktonic foraminiferal assemblages, so reworking obscures the record of the onset of the event (Fig. F7). On the contrary, in Hole 1212B, characterized by lower magnetic susceptibility values and a less dissolved planktonic foraminiferal assemblage, the onset of the event occurs gradually: the beginning of the sharp increase in magnetic susceptibility seems to precede both the deposition of phillipsite and the faunal change. Moreover, the lower abundance of phillipsite in Hole 1212B compared to the other holes might be related to a different depositional environment, as is also suggested by the lighter color of the sediment (see Fig. F7).

The end of the event in all holes occurs more gradually than the onset and coincides with a decrease in magnetic susceptibility, the disappearance of phillipsite, and a sharp increase in the abundance of *I. albeari*.

F7. Main features characterizing the early late Paleocene event at Shatsky Rise, p. 18.

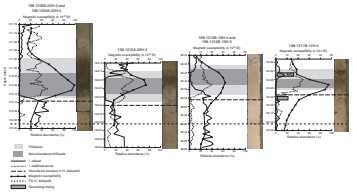

The dissolution event registered by the planktonic foraminiferal assemblages is supported by a decrease in carbonate content (Bralower, Premoli Silva, Malone, et al., 2002) and the presence of the clay-rich interval containing phillipsite and fish teeth. Phillipsite is interpreted as an alteration product of tephra (volcanic ash), especially basaltic glass, at the seafloor or during shallow burial; it replaces volcanic material in slow-sedimentation environments (Rothwell, 1989; Kastner, 1999). Therefore, the presence of abundant crystals of phillipsite and fish teeth suggests slow sedimentation or intervals of seafloor exposure. This is consistent with the pervasive dissolution of carbonate, which occurs when sites are located close to the lysocline depth range or close to the carbonate compensation depth (CCD).

Biostratigraphy suggests that the early late Paleocene event (~58.4 Ma) is of short duration (<1 m.y.). The thin clay-rich layer found in this interval is comparable to the Paleocene/Eocene Thermal Maximum (PETM) (~55.5 Ma); both events involved abrupt shoaling of the lysocline and CCD. PETM carbonate dissolution likely resulted from bottom water oxidation of methane released from sedimentary methane hydrate reservoirs to CO_2 (Dickens et al., 1995, 1997); the cause of the early late Paleocene event is unknown and further investigation is required. At Shatsky Rise, these short-term events seem to be superimposed on a long-term record of CCD variation. In fact, the Paleogene sedimentary record from Sites 1209–1212 is strongly cyclic. The identification of low-amplitude fluctuations in the magnetic susceptibility and color reflectance records highlights the occurrence of episodic dissolution events resulting from periodic lysoclinal and CCD shoaling that perturbated Paleogene carbonate deposition. Such cyclicity suggests the possibility of orbitally controlled lysocline depth changes, probably related to variations in surface water productivity and/or deepwater mass composition (Bralower, Premoli Silva, Malone, et al., 2002).

In the studied samples the original faunal composition is overprinted by dissolution, so no clear evidence of variable surface water productivity is observed. The hypothesis of a shoaling lysocline fits well with the decrease in thickness of the clay-rich layer with depth (Table **T1**), which indicates more condensed sedimentation in the deeper sites that were closer to the CCD. The occurrence of an environmental perturbation is also confirmed by the composition of the planktonic foraminiferal assemblages. For instance, the absence of both surface- and thermocline-dwelling taxa in the clay-rich layer (except for the dissolution-resistant igorinids) is a reasonable consequence of significant shoaling of the lysocline, so a high percentage of taxa dissolved while they settled through the water column. The assemblage changes might also be the result of changing deepwater circulation and shoaling of the boundary between the warm surface water and the deep cold water, the latter being more corrosive.

The assemblages consist mainly of low-latitude tropical and subtropical symbiont-bearing igorinids, which are believed to have occupied a depth habitat between the shallower photosymbiotic morozovellids and the deeper asymbiotic subbotinids (Berggren and Norris, 1997). However, the abundance of igorinids, as well as the common occurrence in the shallower holes of *I. pusilla* "high trochospire" and *I. albeari* "chubby" (morphotypes of *I. pusilla* and *I. albeari,* respectively), could be interpreted as a morphologic response to a decrease in surface water productivity. Reduced nutrient supply could have caused an increase in species competition so that the igorinids modified their morphologies

to the nutrient-limited mesotrophic environment. Moreover, such faunal variations might reflect the difficulty of adapting to changes in water mass owing to modification of deepwater circulation that enhanced dissolution on the seafloor. Additional data on the ecological affinities of the igorinids species, especially *I. albeari,* require further study.

In conclusion, high-resolution quantitative analysis of the planktonic foraminiferal assemblages in the interval surrounding the clay-rich ooze layer reveals significant changes in faunal composition, even though the original faunal composition was altered by dissolution, which affected a large section of the water column. A possible cause of the increased dissolution on the seafloor could be attributed to a change in carbonate solubility, probably related to changes in deep-water circulation over Shatsky Rise and/or variation in surface water productivity, either of which could have caused an abrupt shoaling in the depth of the lysocline and CCD.

ACKNOWLEDGMENTS

I thank the Co-Chief Scientists Timothy J. Bralower and Isabella Premoli Silva and all the scientific participants of ODP Leg 198 for their partnership during the cruise. I also warmly thank the crew members and the shipboard staff for their support. I am indebted and very grateful to Ursula Röhl, who kindly processed the foraminifer samples at the University of Bremen, Germany. Thanks also to Isabella Premoli Silva and Timothy J. Bralower, whose comments and suggestions significantly improved the manuscript. I gratefully acknowledge the critical and thorough reviews by R.K. Olsson and D. Clay Kelly. This research used samples and/or data provided by the Ocean Drilling Program (ODP). ODP is sponsored by the U.S. National Science Foundation (NSF) and participating countries under management of Joint Oceanographic Institutions (JOI), Inc. Funding for this research was provided by MIUR-COFIN 2001 to I.P.S.

REFERENCES

Berggren, W.A., Kent, D.V., Swisher, C.C., III, and Aubry, M.-P., 1995. A revised Cenozoic geochronology and chronostratigraphy. *In* Berggren, W.A., Kent, D.V., Aubry, M.-P., and Hardenbol, J. (Eds.), *Geochronology, Time Scales and Global Stratigraphic Correlation*. Spec. Publ.—SEPM (Soc. Sediment. Geol.), 54:129–212.

Berggren, W.A., and Norris, R.D., 1997. Biostratigraphy, phylogeny and systematics of Paleocene trochospiral planktic foraminifera. *Micropaleontology,* 43 (Suppl. 1):1–116.

Boersma, A., and Premoli-Silva, I., 1983. Paleocene planktonic foraminiferal biogeography and the paleoceanography of the Atlantic Ocean. *Micropaleontology,* 29:355–381.

Bralower, T.J., Premoli Silva, I., and Malone, M.J., 2002. New evidence for abrupt climate change in the Cretaceous and Paleogene: an Ocean Drilling Program expedition to Shatsky Rise, Northwest Pacific. *Geol. Soc. Am. Today,* 12(11):4–10.

Bralower, T.J., Premoli Silva, I., Malone, M.J., et al., 2002. *Proc. ODP, Init. Repts.,* 198 [CD-ROM]. Available from: Ocean Drilling Program, Texas A&M University, College Station TX 77845-9547, USA.

Dickens, G.R., O'Neil, J.R., Rea, D.K., and Owen, R.M., 1995. Dissociation of oceanic methane hydrate as a cause of the carbon isotope excursion at the end of the Paleocene. *Paleoceanography,* 10:965–971.

Dickens, G.R., Castillo, M.M., and Walker, J.G.C., 1997. A blast of gas in the latest Paleocene: simulating first-order effects of massive dissociation of oceanic methane hydrate. *Geology,* 25:259–262.

Kastner, M., 1999. Oceanic minerals: their origin, nature of their environment, and significance. *Proc. Natl. Acad. Sci. USA,* 96:3380–3387.

Luterbacher, H.P., 1964. Studies in some *Globorotalia* from the Paleocene and lower Eocene of the Central Apennines. *Eclogae Geol. Helv.,* 57(2):631–730.

Olsson, R.K., Hemleben, C., Berggren, W.A., and Huber, B.T. (Eds.), 1999. *Atlas of Paleocene Planktonic Foraminifera*. Smithson. Contrib. Paleobiol., Vol. 85.

Rothwell, R.G., 1989. *Minerals and Mineraloids in Marine Sediments: An Optical Identification Guide:* Basking, UK (Elsevier Appl. Sci. Publ.).

APPENDIX

Taxonomic List

This Appendix contains a taxonomic list of all planktonic foraminifers cited in the text, listed in the distribution charts (Tables T2, T3, T4, T5), and illustrated in Plates P1, P2, and P4 and arranged in alphabetic order by genus and species. Comments are included for some species to clarify the taxonomic concepts used in this study and to report significant morphological features observed in the assemblages. The generic and specific concepts follow Luterbacher (1964), Boersma and Premoli Silva (1983), Berggren and Norris (1997), Olsson et al. (1999), and references therein.

Acarinina Subbotina, 1953.

Acarinina mckannai (White) = *Globigerina mckannai* White, 1928.

Acarinina nitida (Martin) = *Globigerina nitida* Martin, 1943.

Acarinina strabocella (Loeblich and Tappan) = *Globorotalia strabocella* Loeblich and Tappan, 1957.

Acarinina subsphaerica (Subbotina) = *Globigerina subsphaerica* Subbotina, 1947.

Globanomalina Haque, 1956, emended.

Globanomalina imitata (Subbotina) = *Globorotalia imitata* Subbotina, 1953.

Globanomalina pseudomenardii (Bolli) = *Globorotalia pseudomenardii* Bolli, 1957.

Globanomalina ehrenbergi (Bolli) = *Globorotalia ehrenbergi* Bolli, 1957.

Igorina Davidzon, 1976.

Igorina albeari (Cushman and Bermudez) = *Globorotalia albeari* Cushman and Bermudez, 1949.

Igorina albeari "chubby"

Remarks: The specimens included in this group seem to be an intermediate form between *Igorina pusilla* and *I. albeari*. The inferred relationship with *I. pusilla* is supported by having similar compressed chambers and strongly curved and slightly depressed sutures on the spiral side. On the other hand, this form resembles *I. albeari* in having a strongly biconvex test, a circular profile, and a low interior marginal aperture with an arch extending toward the peripheral margin but differs in lacking the peripheral keel. This morphotype has previously been reported and illustrated by Berggren and Norris (1997) as *I. albeari* from ODP Hole 758A.

Igorina pusilla (Bolli) = *Globorotalia pusilla pusilla* Bolli, 1957.

Igorina pusilla "high trochospire"

Remarks: This group includes the specimens of *I. pusilla* characterized by having a high trochospire. Similar morphotypes are illustrated by Olsson et al. (1999) from ODP Hole 761B (Wombat Plateau, Indian Ocean).

Igorina tadjikistanensis (Bykova) = *Globorotalia tadjikistanensis* Bykova, 1953.

Morozovella McGowran in Luterbacher, 1964.

Morozovella acuta (Toulmin) = *Globorotalia wilcoxensis* Cushman and Ponton var. *acuta* Toulmin, 1941.

Morozovella acutispira (Bolli and Cita) = *Globorotalia acutispira* Bolli and Cita, 1960.

Morozovella aequa (Cushman and Renz) = *Globorotalia crassata* Cushman var. *aequa* Cushman and Renz, 1942.

Morozovella angulata (White) = *Globigerina angulata* White, 1928.

Morozovella apanthesma (Loeblich and Tappan) = *Globorotalia apanthesma* Loeblich and Tappan, 1957.

Morozovella conicotruncata (Subbotina) = *Globorotalia conicotruncata* Subbotina, 1947.

Morozovella occlusa (Loeblich and Tappan) = *Globorotalia occlusa* Loeblich and Tappan, 1957.

Morozovella pasionensis (Bermudez) = *Pseudogloborotalia pasionensis* Bermudez, 1961.

Morozovella praeangulata (Blow) = *Globorotalia praeangulata* Blow, 1979.

Morozovella velascoensis (Cushman) = *Pulvinulina velascoensis* Cushman, 1925.

Praemurica Olsson, Hemleben, Berggren, and Liu, 1992 *Praemurica inconstans* (Subbotina) = *Globigerina incostans* Subbotina, 1953.

Praemurica praecursoria (Morozova) = *Acarinina praecursoria* Morozova, 1957.

Praemurica uncinata (Bolli) = *Globorotalia uncinata* Bolli, 1957.

Schackoina Thalmann, 1932.

Subbotina Brotzen and Pozaryska, 1961.

Subbotina triangularis White, *Globigerina triangularis* White, 1928.

Subbotina triloculinoides (Plummer) = *Globigerina triloculinoides* Plummer, 1926.

Figure F1. A. Paleogeographic reconstruction (early late Paleocene at 58.4 Ma) showing the location of Shatsky Rise. **B.** Bathymetric map of Shatsky Rise showing location of Leg 198 sites.

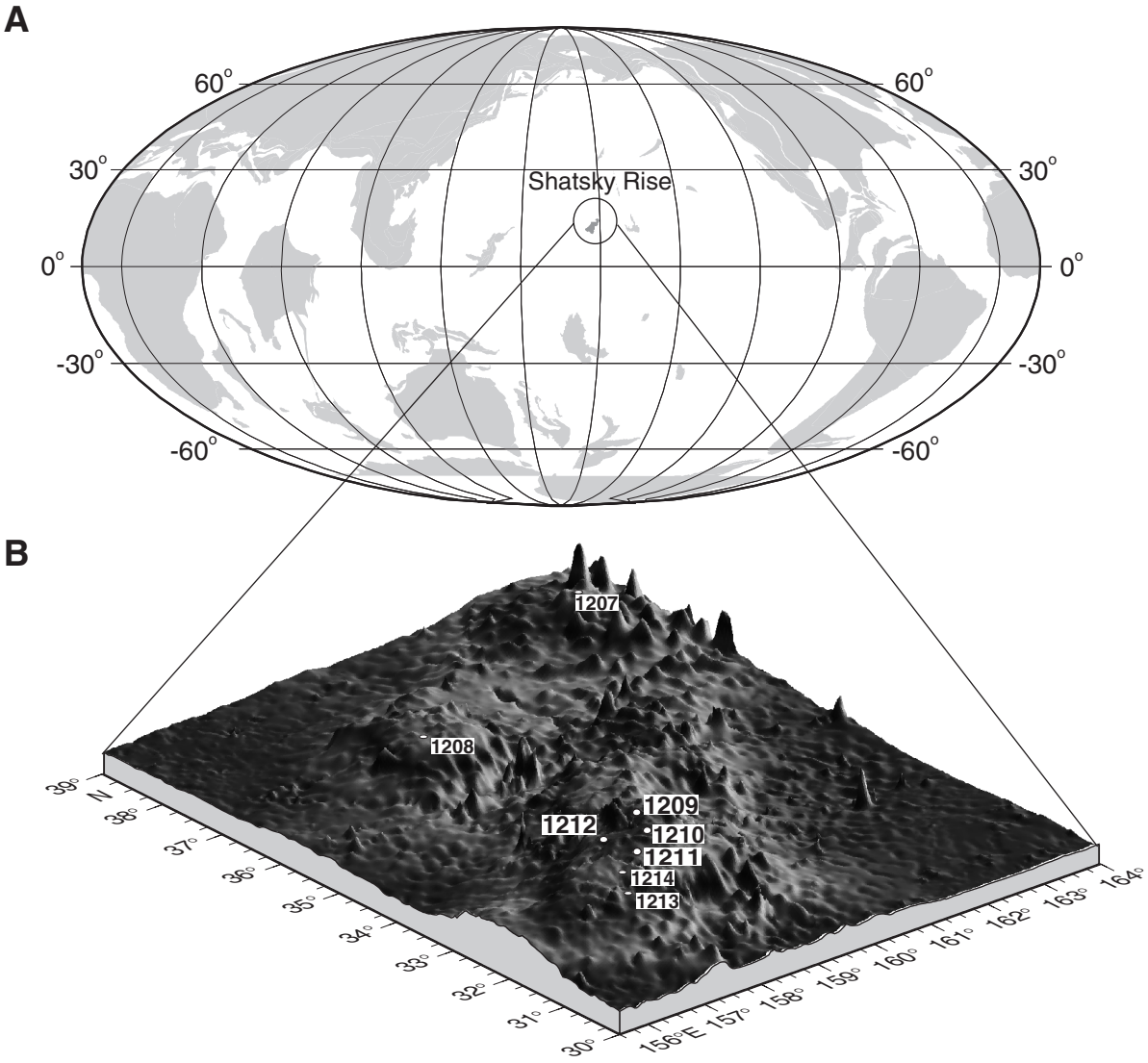

Figure F2. Correlation between number of species and magnetic susceptibility in Holes 1209A, 1210A, 1212B, 1211B.

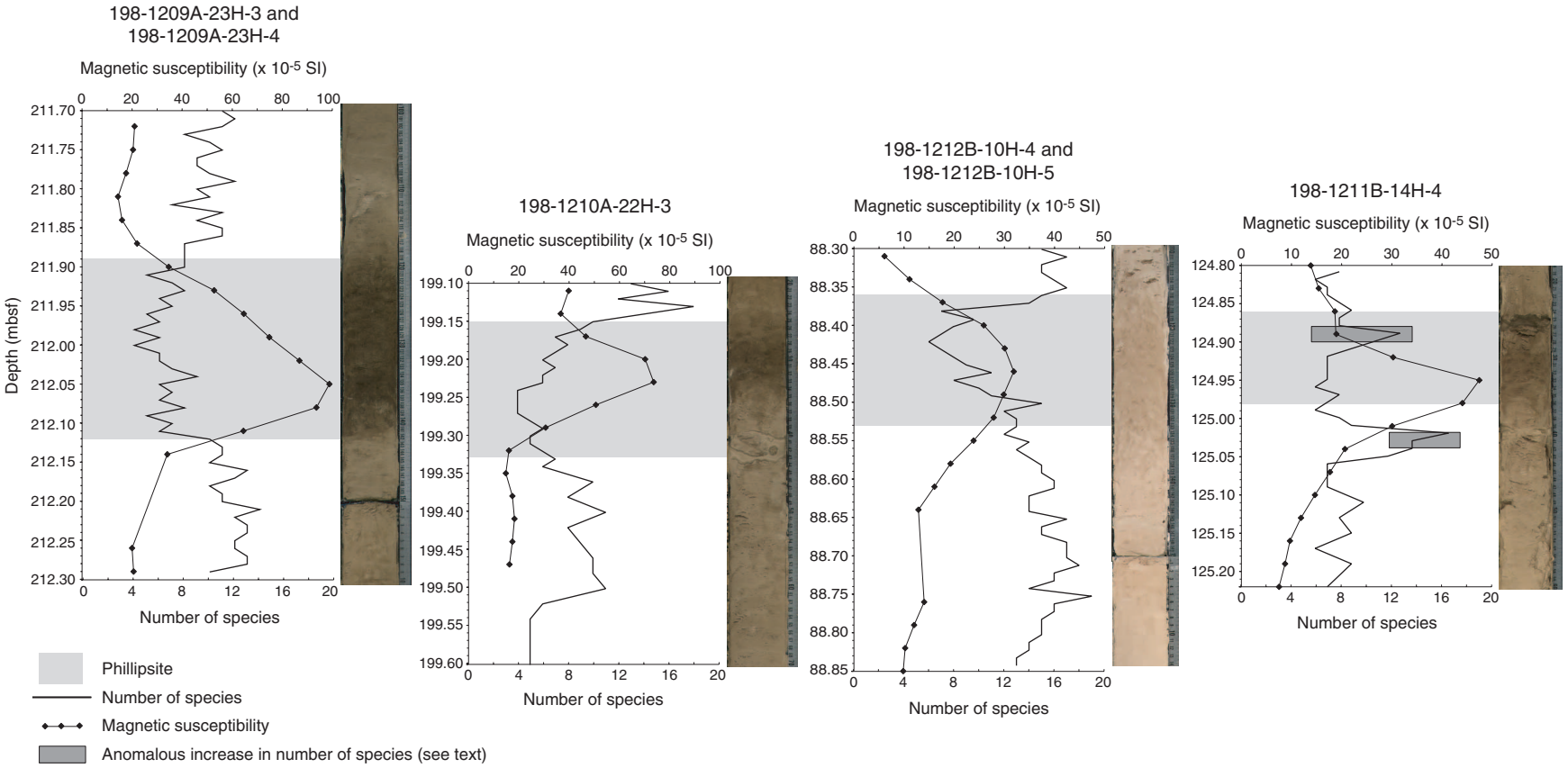

Figure F3. *Igorina, Morozovella,* and *Acarinina* relative abundances (percent of total specimens). FO = first occurrence.

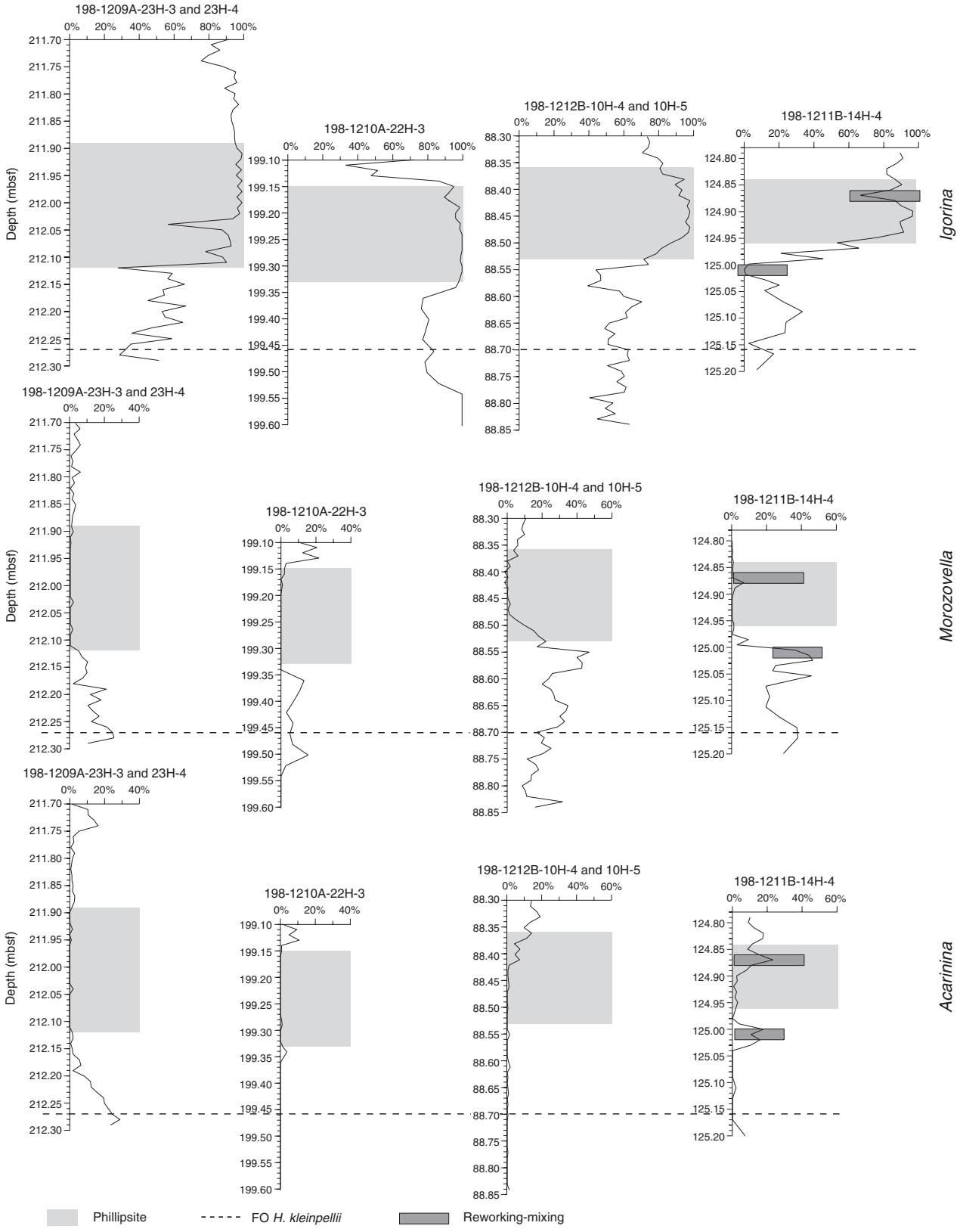

Figure F4. *Globanomalina, Chiloguembelina,* and *Subbotina* relative abundances (percent of total specimens). FO = first occurrence.

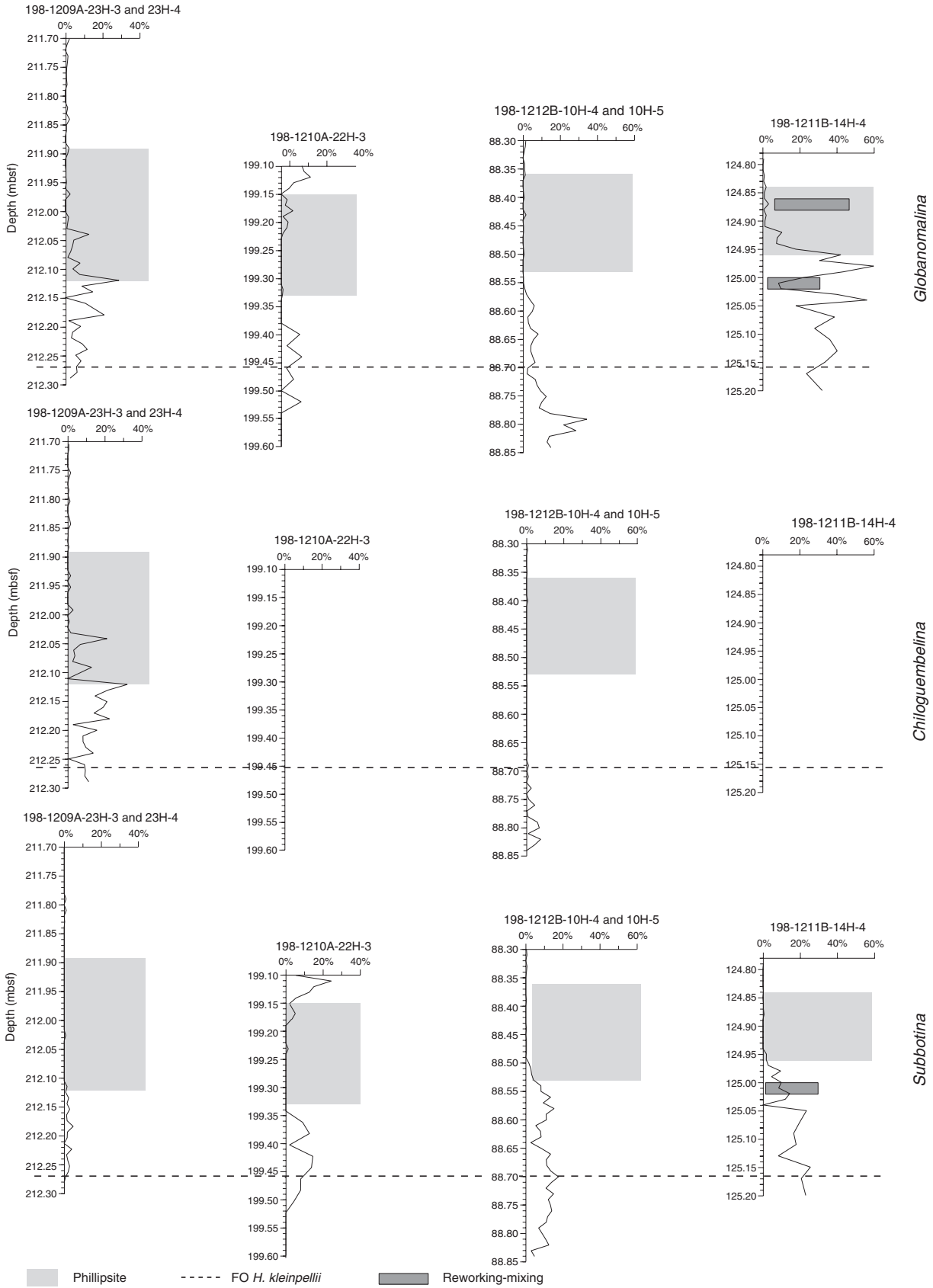

Figure F5. *Igorina tadjikistanensis, Igorina albeari,* and *Igorina pusilla* relative abundances (percent of total specimens). FO = first occurrence.

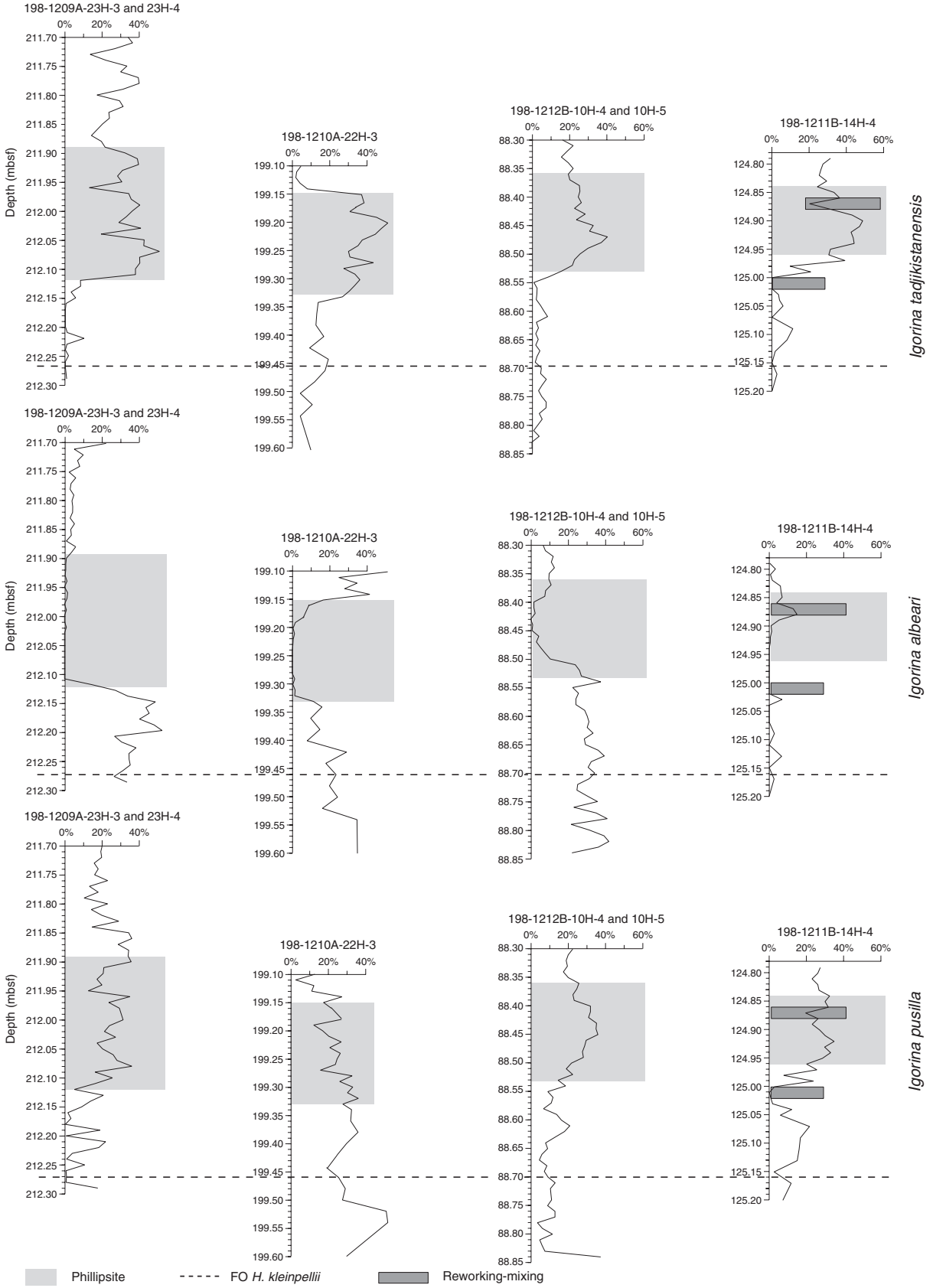

Figure F6. *Igorina pusilla* "high trochospire" and *Igorina albeari* "chubby" relative abundances (percent of total specimens). FO = first occurrence.

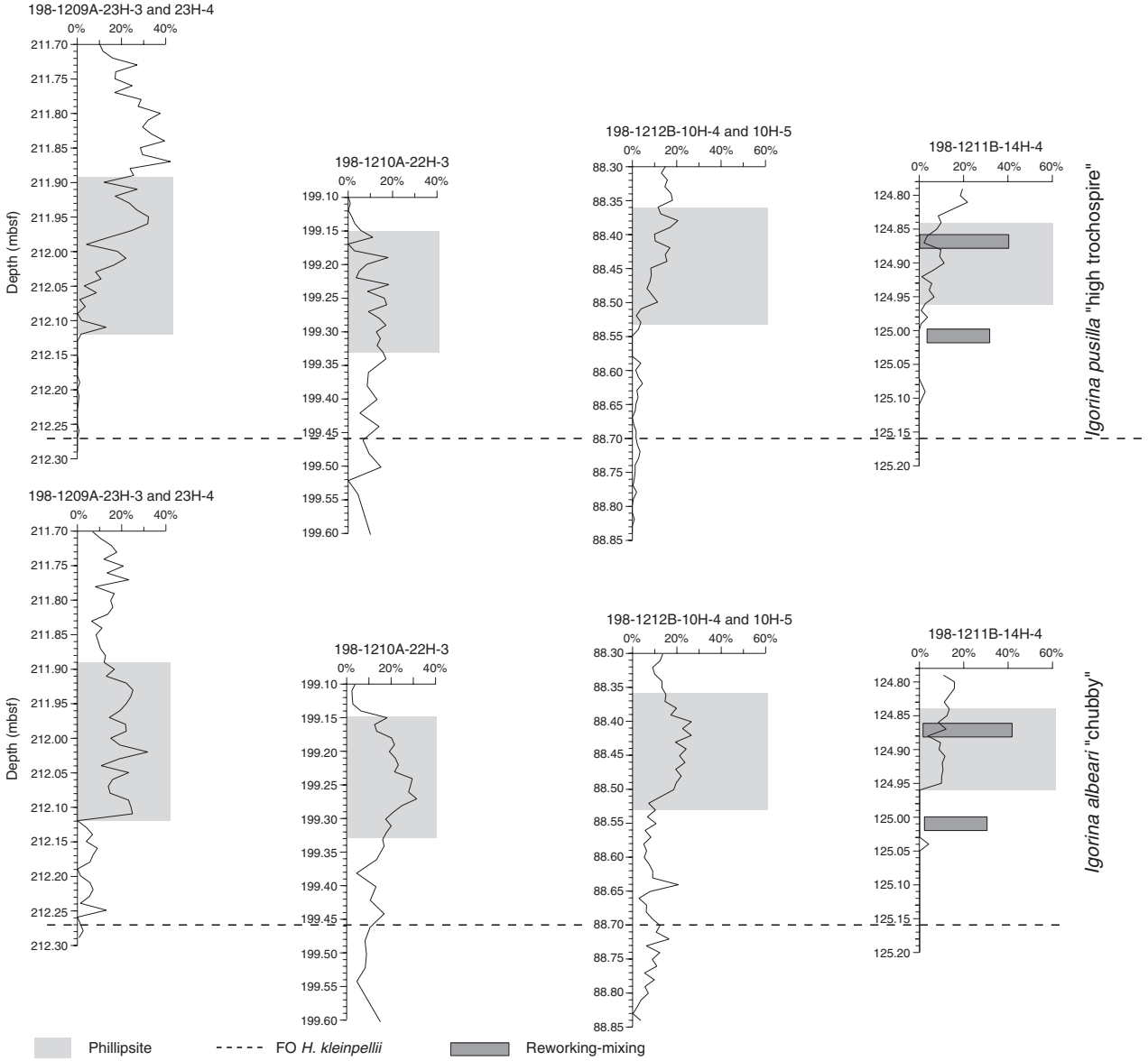

Figure F7. Summary of the main features characterizing the early late Paleocene event at Shatsky Rise. Max = maximum. FO = first occurrence.

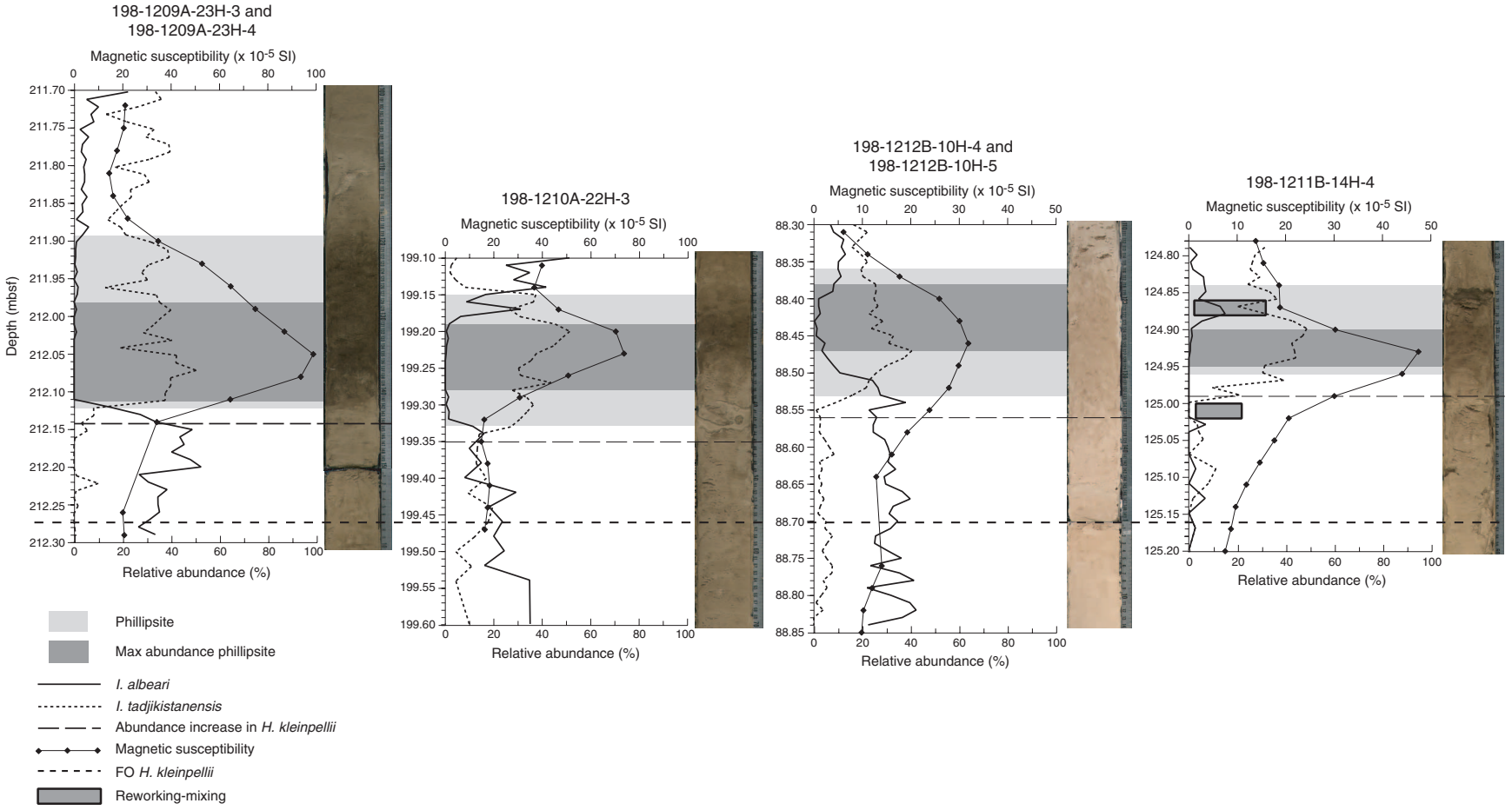

Table T1. Selected samples from Leg 198 holes.

Core, section, interval (cm)	Water depth (m)	Studied interval depth (mbsf)	Clay-rich layer depth (mbsf)	Clay-rich layer thickness (cm)	Clay-rich layer color
198-1209A-23H-3, 100–101 to 23H-4, 9–10	2387	211.7 to 212.29	211.89 to 212.12	23	Dark brown
198-1210A-22H-3, 20–21 to 22H-3, 44–45	2573	199.10 to 199.35	199.15 to 199.33	18	Dark brown
198-1212B-10H-4, 110–111 to 10H-5, 14–15	2681	88.30 to 88.84	88.36 to 88.53	17	Light brown
198-1211B-14H-4, 19–20 to 14H-4, 45–46	2907	124.79 to 125.05	124.85 to 124.96	11	Dark brown

Table T2. Assemblage count data for planktonic foraminifers, Hole 1209A. (**See table notes.** Continued on next page.)

Core, section, interval (cm)	Depth (mbsf)	*Benthic foraminifers*	*Igorina tadjikistanensis*	*Igorina pusilla*	*Igorina albeari*	*Acarinina subsphaerica*	*Morozovella occlusa*	*Morozovella apanthesma*	*Igorina pusilla* "high trochospire"	*Igorina albeari* "chubby"	*Morozovella pasionensis*	*Globanomalina* sp.	*Chiloguembelina* sp.	*Globigerinelloides* sp.	*Acarinina* sp.	*Morozovella velascoensis*	*Acarinina mckannai*	*Morozovella aequa*	*Subbotina triloculinoides*	*Subbotina* sp.	*Globanomalina pseudomenardii*	*Morozovella acuta*	*Morozovella acutispira*	Total specimens	Comments
198-1209A-																									
23H-3, 100–101	211.70	F	204	61	19	4	5	4	?	?		7	2	1										309	Large-sized highly fragmented
23H-3, 101–102	211.71		110	58	16	31	8	6	35	32	3	3	2		1									305	Large-sized fragmented
23H-3, 102–103	211.72		87	64	33	34	2	1	52	50	3					1	?							328	Large-sized fragmented
23H-3, 103–104	211.73		36	42	19	38			73	48	11	4												271	Large-sized fragmented
23H-3, 104–105	211.74		53	43	20	40		3	42	29	7	3				4								244	Small-sized dominant
23H-3, 105–106	211.75		80	38	6	13	2	3	41	50	3	2	4											242	Small-sized dominant
23H-3, 106–107	211.76		89	68	18	6		1	74	40		2	2											300	
23H-3, 107–108	211.77		112	37	10	7		2	48	66	2	2												286	
23H-3, 108–109	211.78		119	53	9	2		1	86	24		3	2					1						300	
23H-3, 109–110	211.79		86	28	14	7	12	2	76	46	2		1		1				3					278	Large-sized fragmented
23H-3, 110–111	211.80		51	68	12	5	2		112	45	1		4											300	
23H-3, 111–112	211.81		73	35	11	3	3		80	40	2							1	3					251	
23H-3, 112–113	211.82		93	59	13	2			88	41		4												300	
23H-3, 113–114	211.83		70	86	9	4	3		100	19	3	2	3						1					300	
23H-3, 114–115	211.84		71	43	16	4			118	33	3	7	5											300	Small-sized dominant
23H-3, 115–116	211.85		60	102	10	6	1	2	85	25	6	2	1											300	
23H-3, 116–117	211.86		51	107	11	5	3	3	88	28	1	2	1											300	
23H-3, 117–118	211.87		42	85	3	9	1	3	126	31														300	
23H-3, 118–119	211.88		58	102	18	8			71	38	3		2											300	
23H-3, 119–120	211.89		64	101	11	4			76	36	2	6												300	R phillipsite
23H-3, 120–121	211.90		96	106	3		1	4	36	50		4												300	Small-sized dominant, F phillipsite
23H-3, 121–122	211.91		116	62	2				81	39														300	Small-sized dominant, F phillipsite
23H-3, 122–123	211.92		118	61	2	1	1		51	66														300	
23H-3, 123–124	211.93		92	51	1	5			70	75		1	5											300	C phillipsite
23H-3, 124–125	211.94		84	59	4				80	72		1												300	C phillipsite
23H-3, 125–126	211.95		91	37		3			96	66		2	5											300	R phillipsite
23H-3, 126–127	211.96		39	105	5				96	58														303	Small-sized dominant, C phillipsite
23H-3, 127–128	211.97		102	70	4				73	43		8												300	Small-sized dominant, C phillipsite
23H-3, 128–129	211.98	C	106	87					42	65														300	R small-sized plank, A phillipsite
23H-3, 129–130	211.99	C	40	30	1				4	22			3											100	R small-sized plank, A phillipsite
23H-3, 130–131	212.00	C	36	31					18	15														100	R small-sized plank, AA phillipsite
23H-3, 131–132	212.01	A	36	26					24	21		2	1											110	R small-sized plank, AA phillipsite
23H-3, 132–133	212.02	A	86	63	3?				49	95		4												300	R small-sized plank, AA phillipsite
23H-3, 133–134	212.03	C	45	30			2		9	21		1	2						1					111	R small-sized plank, AA phillipsite
23H-3, 134–135	212.04	A	9	8		1			5	5		6	10	3										47	VR small-sized plank, AA phillipsite
23H-3, 135–136	212.05	C	55	26					4	30		6	9											130	R small-sized plank, A phillipsite
23H-3, 136–137	212.06	C	64	39					13	24		6	5	1										152	VR small-sized plank, AA phillipsite
23H-3, 137–138	212.07	A	51	28					1	14		3	4											101	R small-sized plank, A phillipsite

Table T2 (continued).

Core, section, interval (cm)	Depth (mbsf)	*Benthic foraminifers*	*Igorina tadjikistanensis*	*Igorina pusilla*	*Igorina albeari*	*Acarinina subsphaerica*	*Morozovella occlusa*	*Morozovella apanthesma*	*Igorina pusilla* "high trochospire"	*Igorina albeari* "chubby"	*Morozovella pasionensis*	*Globanomalina* sp.	*Chiloguembelina* sp.	*Globigerinelloides* sp.	*Acarinina* sp.	*Morozovella velascoensis*	*Acarinina mckannai*	*Morozovella aequa*	*Subbotina triloculinoides*	*Subbotina* sp.	*Globanomalina pseudomenardii*	*Morozovella acuta*	*Morozovella acutispira*	Total specimens	Comments
23H-3, 138–139	212.08	C	57	51				2	5	21		2	4	1										143	R small-sized plank, A phillipsite
198-1209A-																									
23H-3, 139–140	212.09	F	40	16						23		8	13											100	R small-sized plank, A phillipsite
23H-3, 140–141	212.10	C	64	43					3	41		7	11	1										170	R small-sized plank, A phillipsite
23H-3, 141–142	212.11	A	38	16					13	25		8		1										101	VR small-sized plank, AA phillipsite
23H-3, 142–143	212.12	C	5	3	9	1	3		1			18	20	1					1					62	Small-sized plank, small residue
23H-3, 143–144	212.13		20	50	67	5	5	8		10	3	22	53						2					245	Small-sized plank, highly fragmented
23H-3, 144–145	212.14	C	5	22	55	1	11	5		11		24	24						1	3				162	Small-sized plank, highly fragmented
23H-3, 145–146	212.15	C	7	11	62	2	7	3		5	1		27						2					127	Small-sized plank, highly fragmented
23H-3, 146–147	212.16	C	1	4	132	6	7	18	1	27	4	33	58	2						9				302	Highly fragmented
23H-3, 147–148	212.17	F		9	137	11	4	9		21	8	48	43	1	6					4				301	Highly fragmented
23H-3, 148–149	212.18				50	2	1			7	1	26	28	1	6					2				124	Highly fragmented, small residue
23H-3, 149–150	212.19			19	49	2	14	6	1		1	2	3						3	2				102	Highly fragmented
23H-4, 0–1	212.20	F		1	119	10	6	11		3	9	19	36		9					4				227	Highly fragmented
23H-4, 1–2	212.21	C	3	65	81	36	24	21	2	17	8	11	25	2					5		1			301	Highly fragmented
23H-4, 2–3	212.22		30	54	92	37	12	6	1	21	3	10	25					9						300	Highly fragmented
23H-4, 3–4	212.23		2	9	93	27	8	14		13	9	21	24		11					10	1			242	Highly fragmented
23H-4, 4–5	212.24			2	105	46	24	13		4	11	36	42	1	13			2		4				303	Highly fragmented
23H-4, 5–6	212.25		5	31	104	60	13	14		39	3	17	2					6		6				300	Highly fragmented
23H-4, 6–7	212.26			1	108	68	30	14	2		14	26	28			3		3		9				306	Highly fragmented
23H-4, 7–8	212.27			2	98	73	33	16		4	18	19	30	1	4			9		7				314	Highly fragmented, F large-sized plank
23H-4, 8–9	212.28		1	1	83	90	27	29		8	10	20	29							2		10	2?	312	
23H-4, 9–10	212.29		1	26	50	35	6			1	8	4	17					1?						149	Highly fragmented, small residue

Notes: AA = very abundant, A = abundant, C = common, F = few, R = rare, VR = very rare. plank = planktonic foraminifers.

Table T3. Assemblage count data for planktonic foraminifers, Hole 1210A.

Core, section, interval (cm)	Depth (mbsf)	*Igorina tadjikistanensis*	*Igorina pusilla*	*Igorina albeari*	*Acarinina subsphaerica*	*Igorina pusilla* "high trochospire"	*Igorina albeari* "chubby"	*Globanomalina* sp.	*Subbotina* sp.	*Chiloguembelina* sp.	*Morozovella occlusa*	*Morozovella apanthesma*	*Globigerinelloides* sp.	*Globanomalina pseudomenardii*	*Morozovella pasionensis*	*Morozovella aequa*	*Morozovella acuta*	*Morozovella acutispira*	*Morozovella velascoensis*	*Acarinina nitida*	Total specimens	Comments
198-1210A-																						
22H-3, 20–21	199.10	13	36	142	3		10	28	15		6	13		3	2		4		2		277	Highly fragmented, small-sized dominant, R phillipsite
22H-3, 21–22	199.11	8	9	83	28	3	7	29	81		21	21		12	6	5	4	11		3	331	Fragmented, small-sized dominant
22H-3, 22–23	199.12	6	38	106	15		7	42	46		12	18		6			5	3			304	Highly fragmented, small-sized dominant
22H-3, 23–24	199.13	13	35	87	26	5	8	18	39	1	28	15		3	1	2	9	11	1	7	309	Highly fragmented, small-sized dominant, R phillipsite
22H-3, 24–25	199.14	25	84	127	2	9	19	13	17		1	2			1	2	1	2			305	Highly fragmented, small-sized dominant, R phillipsite
22H-3, 25–26	199.15	112	53	50	2	17	54		6		1	3			2						300	Highly fragmented, small-sized dominant, R phillipsite
22H-3, 26–27	199.16	112	67	27		34	38	10	14		5	1									308	Highly fragmented, small-sized dominant, R phillipsite
22H-3, 27–28	199.17	12	5	14			6		6				1	1							45	Highly fragmented, R plank, C phillipsite
22H-3, 28–29	199.18	34	30	7		3	22	7	6			1									110	Highly fragmented, R plank, C phillipsite
22H-3, 29–30	199.19	136	37	5		54	64	3			1										300	Highly fragmented, small-sized dominant, A phillipsite
22H-3, 30–31	199.20	111	37	1		18	41	8													216	Highly fragmented, small-sized dominant, A phillipsite
22H-3, 31–32	199.21	77	33	2		8	35	5		1											161	Highly fragmented, R/F plank, A phillipsite
22H-3, 32–33	199.22	87	53	1		7	45	2													195	Highly fragmented, R/F plank, A phillipsite
22H-3, 33–34	199.23	113	63	1		55	64		4												300	Highly fragmented, R/F plank, AA phillipsite
22H-3, 34–35	199.24	106	80			26	88														300	Highly fragmented, R/F plank, AA phillipsite
22H-3, 35–36	199.25	91	75			49	86														301	Highly fragmented, R/F plank, AA phillipsite, fish teeth
22H-3, 36–37	199.26	93	72			52	83														300	Highly fragmented, F/C plank, AA phillipsite, fish teeth
22H-3, 37–38	199.27	131	48			27	94														300	Highly fragmented, small-sized dominant, A phillipsite
22H-3, 38–39	199.28	83	99		2	42	74														300	Highly fragmented, small-sized dominant, A phillipsite
22H-3, 39–40	199.29	101	79	4	3	51	62														300	Highly fragmented, small-sized dominant, C phillipsite
22H-3, 40–41	199.30	109	100	1		38	52														300	Highly fragmented, small-sized dominant, C phillipsite
22H-3, 41–42	199.31	107	97	5		46	63														318	Highly fragmented, small-sized dominant, F phillipsite
22H-3, 42–43	199.32	92	109	4		39	53	3													300	Highly fragmented, small-sized dominant, R/F phillipsite
22H-3, 43–44	199.33	81	84	34	4	47	48	2													300	Highly fragmented, small-sized dominant, R phillipsite
22H-3, 44–45	199.34	42	98	48	11	51	50														300	Highly fragmented, small-sized dominant

Notes: AA = very abundant, A = abundant, C = common, F = few, R = rare. plank = planktonic foraminifers.

Table T4. Assemblage count data for planktonic foraminifers, Hole 1211B.

Core, section, interval (cm)	Depth (mbsf)	*Igorina tadjikistanensis*	*Igorina pusilla*	*Morozovella occlusa*	*Subbotina* sp.	*Morozovella conicotruncata*	*Morozovella angulata*	*Morozovella apanthesma*	*Igorina albeari* "chubby"	*Globanomalina* sp.	*Igorina albeari*	*Acarinina subsphaerica*	*Globanomalina pseudomenardii*	*Acarinina nitida*	*Morozovella pasionensis*	*Morozovella velascoensis*	*Praemurica uncinata*	*Morozovella praeangulata*	*Acarinina strabocella*	*Praemurica inconstans*	*Igorina pusilla* "high trochospire"	*Morozovella acuta*	*Morozovella acutispira*	*Acarinina mckannai*	*Morozovella aequa*	Total specimens	Comments
198-1211B-																											
14H-4, 19–20	124.79	94	82		1				32	1	1	30									59					300	Slightly fragmented, small-sized dominant
14H-4, 20–21	124.80	82	78						47		10	27									56					300	Slightly fragmented, small-sized dominant
14H-4, 21–22	124.81	79	69	1					47		2	37									66					301	Slightly fragmented, small-sized dominant
14H-4, 22–23	124.82	76	78						40	2	5	53									46					300	Slightly fragmented, small-sized dominant
14H-4, 23–24	124.83	88	80					2	33	1	18	52									26					300	Slightly fragmented, small-sized dominant
14H-4, 24–25	124.84	73	97		1			1	40	5	19	34									30					300	Small-sized dominant, R phillipsite
14H-4, 25–26	124.85	100	90	1					37	2	21	26									24					301	Small-sized dominant, R phillipsite
14H-4, 26–27	124.86	109	95		1				25	2	12	45									11					300	Small-sized dominant, R phillipsite
14H-4, 27–28	124.87	61	59	9	1			5	36	8	39	70	1		6						7		1			303	Small-sized dominant, R phillipsite
14H-4, 28–29	124.88	96	79	1	2			3	11	1	45	33				1					30					302	Small-sized dominant, R phillipsite
14H-4, 29–30	124.89	129	69	1					28	5	16	23			1						28					300	Small-sized dominant, F phillipsite
14H-4, 30–31	124.90	146	81						26	3	3	7									34					300	F plank, A phillipsite
14H-4, 31–32	124.91	141	90						34	3	4	8									20					300	F plank, A phillipsite
14H-4, 32–33	124.92	67	55						16	16	1	1									2					158	R plank, AA phillipsite
14H-4, 33–34	124.93	75	51						18	13	1	4									10					172	R plank, AA phillipsite
14H-4, 34–35	124.94	67	50						15	11		2									7					152	R plank, AA phillipsite
14H-4, 35–36	124.95	32	29		2	1			10	18		3									7					102	R plank, AA phillipsite
14H-4, 36–37	124.96	32	21		2			1		44		2									3					105	R plank, AA phillipsite
14H-4, 37–38	124.97	40	26		3					31		1									1					102	R plank, AA phillipsite
14H-4, 38–39	124.98	5	4	2	5	1				31						2					2					52	VR plank, large-sized highly fragmented
14H-4, 39–40	124.99	22	25	1	5					46		4				1					1				1	106	R plank, AA phillipsite
14H-4, 40–41	125.00		9	30	33	12		26		46		8	30		8	20	35	13	25			10	4	25		334	Complete fauna and old (Zone P3)
14H-4, 41–42	125.01			51	31	35	38			17		1	13	26	10	9	81	22	11	17						362	Complete fauna and old (Zone P3)
14H-4, 42–43	125.02		2	37	38	23	38			25		7		21	9	5	30	13	13							261	Complete fauna and old (Zone P3)
14H-4, 43–44	125.03	2	1	2	7	4	9			21	4	2	2	4												58	VR plank, very small residue
14H-4, 44–45	125.04	1	3	2		2		2	1	14																25	VR plank, very small residue
14H-4, 45–46	125.05	1	1	2	4	5	1			3																17	VR plank, very small residue

Notes: AA = very abundant, A = abundant, F = few, R = rare, VR = very rare. plank = planktonic foraminifers.

Table T5. Assemblage count data for planktonic foraminifers, Hole 1212B. (**See table notes.** Continued on next page.)

Core, section, interval (cm)	Depth (mbsf)	*Benthic foraminifers*	*Igorina tadjikistanensis*	*Igorina pusilla*	*Igorina albeari*	*Acarinina subsphaerica*	*Morozovella occlusa*	*Morozovella apanthesma*	*Igorina pusilla* "high trochospire"	*Igorina albeari* "chubby"	*Morozovella pasionensis*	*Globanomalina* sp.	*Chiloguembelina* sp.	*Globigerinelloides* sp.	*Acarinina* sp.	*Morozovella velascoensis*	*Acarinina mckannai*	*Morozovella aequa*	*Subbotina triloculinoides*	*Subbotina* sp.	*Globanomalina pseudomenardii*	*Morozovella acuta*	*Morozovella acutispira*	*Acarinina nitida*	*Morozovella angulata*	*Hedbergella* sp.	*Morozovella conicotruncata*	Total specimens	Comments
198-1212B-																													
10H-4, 110–111	88.30		52	71	21	44	4	1	48	43	10	5				7		2		1		6	5					320	Pyrite, slightly fragmented
10H-4, 111–112	88.31		70	63	25	39	7	2	42	39	5	4	2			5		3		2		3	5	3				319	Pyrite, slightly fragmented
10H-4, 112–113	88.32		59	59	38	48	5	1	50	28	10	2				5		2				1	3	5				316	Fragmented
10H-4, 113–114	88.33		51	63	36	51	5	1	48	32	11					6		2		2		4	4	10				326	Fragmented
10H-4, 114–115	88.34		61	54	40	38	3		55	41	5	2				3		2		1	1	3	3	3				315	Fragmented, R phillipsite
10H-4, 115–116	88.35		69	62	31	29	3	1	57	41	4	2	1			6		1			1	2	3	1				314	Fragmented, R phillipsite
10H-4, 116–117	88.36		60	79	30	40	2	1	36	46	3	3				2					1	2	2	3				310	Highly fragmented, small-sized dominant, F phillipsite
10H-4, 117–118	88.37		63	76	34	33	4	2	40	45	3					2		2				3	4	1				312	Highly fragmented, small-sized dominant, C phillipsite
10H-4, 118–119	88.38		76	67	24	12			62	59								1										301	Highly fragmented, small-sized dominant, A phillipsite
10H-4, 119–120	88.39		78	70	23	22	1	1	52	52						1		1		1	1		2					305	Highly fragmented, small-sized dominant, C phillipsite
10H-4, 120–121	88.40		74	95	5	13			30	79		2	2															300	Highly fragmented, small-sized dominant, A phillipsite
10H-4, 121–122	88.41		79	95	5	21			31	67	2																	300	Highly fragmented, small-sized dominant, A phillipsite
10H-4, 122–123	88.42		68	92	7	3			51	79																		300	Highly fragmented, small-sized dominant, A phillipsite
10H-4, 123–124	88.43		86	106		1	2		45	58		5																303	Highly fragmented, small-sized dominant, A phillipsite
10H-4, 124–125	88.44		71	104	3	1		1	47	72										1								300	Highly fragmented, small-sized dominant, A phillipsite
10H-4, 125–126	88.45		98	107	2	2	1		25	63	1	1																300	Highly fragmented, small-sized dominant, A phillipsite
10H-4, 126–127	88.46		93	89	13	3	2		26	71	1	1				3				1								303	Highly fragmented, small-sized dominant, C phillipsite
10H-4, 127–128	88.47		121	86	9		1		24	58										1			1					301	Highly fragmented, small-sized dominant, C phillipsite
10H-4, 128–129	88.48		112	83	16		1		20	66	1					1				1			2					303	Highly fragmented, small-sized dominant, C phillipsite
10H-4, 129–130	88.49		92	86	24		5		28	60	1	1				3						3	5					308	Fragmented, small-sized dominant, F phillipsite
10H-4, 130–131	88.50		81	68	33	1	4	3	36	58	9	2				3		2		5		6	5					316	Fragmented, R phillipsite
10H-4, 131–132	88.51		75	62	79		12		13	42	8					5		7		9		11	8					331	Fragmented, R phillipsite
10H-4, 132–133	88.52		70	72	85		16	7	6	23	11					5		3		10		6	11					325	Fragmented, R phillipsite
10H-4, 133–134	88.53		53	48	9		40	2	13	34	7					6		3		14		8	9					246	Slightly fragmented
10H-4, 134–135	88.54		29	59	121		14	6	9	21	15									26	1	9	12					322	Slightly fragmented
10H-4, 135–136	88.55		3	27	69	4	26	28		32	13	1	1			7				25		35	36					307	Very slightly fragmented
10H-4, 136–137	88.56		8	34	75		24	23		16	21	3				8		3		39		23	16					293	
10H-4, 137–138	88.57		8	33	75		15	18		25	23	5				16		3		29	1	26	33					310	
10H-4, 138–139	88.58		7	20	75		36	21		15	16	10		1		10		1		47	2	22	27					310	
10H-4, 139–140	88.59		14	42	90		28	2	12	19	6	19				14		1		34		8	18		4			311	
10H-4, 140–141	88.60		20	51	96	2	19	2	5	16	15	16				12		1		35		6	20		1			317	
10H-4, 141–142	88.61		25	62	94	2	17	6	8	22	10	8				2				16		5	18	3	3			301	Fragmented, morozovellids small
10H-4, 142–143	88.62		7	54	92		27	9	14	27	7	9				8				24		7	17		2			304	Fragmented
10H-4, 143–144	88.63		10	37	98	1	24	1	6	26	14	12				7				24		11	22					293	Fragmented
10H-4, 144–145	88.64		6	23	87		8	7	8	62	21	23				16				8	2	11	21					303	Fragmented
10H-4, 145–146	88.65		10	26	88	1	23	19	5	23	14	16				13		2		25	1	17	11		6			300	Slightly fragmented
10H-4, 146–147	88.66		6	17	109	2	23	11	4	8	12	13				10				40		18	16		12			301	Slightly fragmented
10H-4, 147–148	88.67		13	13	122		21	3		19	13	12	1			13				34	1	15	23		6			309	Slightly fragmented

Table T5 (continued).

Core, section, interval (cm)	Depth (mbsf)	*Benthic foraminifers*	*Igorina tadjikistanensis*	*Igorina pusilla*	*Igorina albeari*	*Acarinina subsphaerica*	*Morozovella occlusa*	*Morozovella apanthesma*	*Igorina pusilla* "high trochospire"	*Igorina albeari* "chubby"	*Morozovella pasionensis*	*Globanomalina* sp.	*Chiloguembelina* sp.	*Globigerinelloides* sp.	*Acarinina* sp.	*Morozovella velascoensis*	*Acarinina mckannai*	*Morozovella aequa*	*Subbotina triloculinoides*	*Subbotina* sp.	*Globanomalina pseudomenardii*	*Morozovella acuta*	*Morozovella acutispira*	*Acarinina nitida*	*Morozovella angulata*	*Hedbergella* sp.	*Morozovella conicotruncata*	Total specimens	Comments
10H-4, 148–149	88.68		8	25	98	1	30	6	2	18	6	13				8		6		34	3	17	16		11			302	Slightly fragmented
198-1212B-																													
10H-4, 149–150	88.69		5	20	89		20	8	5	25	9	19	3			1		3		39		20	17		6		1?	289	Slightly fragmented
10H-5, 0–1	88.70		15	27	104	1	5	9	5	37	8	6	1			2		3		53	2	15	10					303	Fragmented
10H-5, 1–2	88.71		14	39	96		21	3	7	32	7	6	3			6		5		42	1	10	10		3		1	306	Slightly fragmented
10H-5, 2–3	88.72		24	32	79		11	6	11	51	9	18				4		1		34	3	18	8		5			314	Slightly fragmented
10H-5, 3–4	88.73		17	33	78		23	5	9	19	8	23	8			10				47	1	16	13		5			315	Slightly fragmented
10H-5, 4–5	88.74		11	34	95		16	5	4	38	4	30				6				38		21	10		3			315	Slightly fragmented
10H-5, 5–6	88.75		16	27	111		10	3	4	27	2	35	4	3		1		1		41	4	7	11		1	2		310	Fragmented
10H-5, 6–7	88.76		24	40	73		17	6	3	34	4	31	14			2				44	1	9	10		4			316	Fragmented
10H-5, 7–8	88.77		23	39	108	1	14	4	1	16	7	27	1			2				36		17	6		6			308	Fragmented
10H-5, 8–9	88.78	C	6	5	64		5	5	3	15	3	22	1			3				17	1	5	1					156	Highly fragmented, small residue
10H-5, 9–10	88.79	C	11	12	44		9	5	1	11	1	70	12			1				14		7	4		1			203	Highly fragmented, small-sized plank dominate
10H-5, 10–11	88.80		5	18	50		5	2		11		34	11	1		2				14	1	2	2		1			159	Highly fragmented, small residue
10H-5, 11–12	88.81		1	5	44		6	1		4	2	30	1	1						12	2	2	1					112	Highly fragmented, small residue
10H-5, 12–13	88.82		4	6	44		7	1	1	2	2	14	8							13	1	1	1					105	Highly fragmented, very small residue
10H-5, 13–14	88.83			5	25		1	7			3	9	3	1						2		5	3		3	2		69	Highly fragmented, very small residue
10H-5, 14–15	88.84			32	19		4	1		3	2	13				1	1			4		3	2		1			86	Highly fragmented, very small residue

Notes: A = abundant, C = common, F = few, R = rare. plank = planktonic foraminifers.

Plate P1. Scanning electron microscope pictures. **1.** *Globanomalina* sp. (Sample 198-1209A-23H-3, 144–145 cm). **2, 3.** *Globanomalina pseudomenardii;* (2a–c) Sample 198-1209A-23H-4, 3–4 cm; (3a–c) Sample 198-1210A-22H-3, 21–22 cm. **4.** *Globanomalina imitata* (Sample 198-1209A-23H-4, 7–8 cm). **5, 8.** *Subbotina velascoensis* (Sample 198-1209A-23H-4, 5–6 cm). **6.** *Subbotina triangularis* (Sample 198-1209A-23H-3, 149–150 cm). **7.** *Subbotina triloculinoides* (Sample 198-1209A-23H-3, 111–112 cm). **9.** *Schackoina* sp. (Sample 198-1209A-23H-3, 140–141 cm).

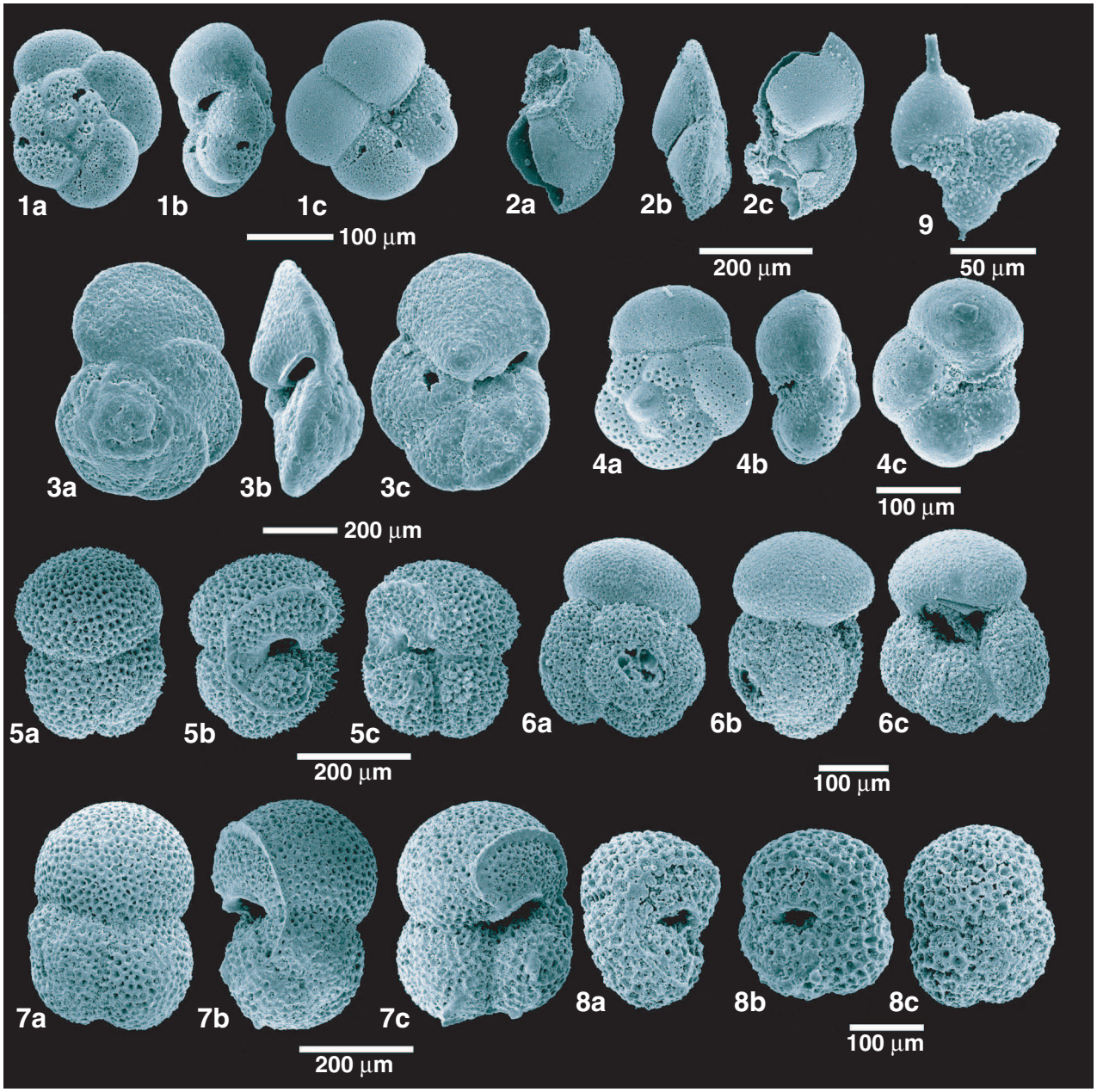

Plate P2. Scanning electron microscope pictures. **1, 2.** *Morozovella pasionensis* (Sample 198-1209A-23H-4, 7–8 cm). **3.** *Morozovella acuta* (Sample 198-1210A-22H-3, 21–22 cm). **4.** *Morozovella velascoensis* (Sample 198-1209A-23H-3, 104–105 cm). **5.** *Morozovella apanthesma* (Sample 198-1209A-23H-3, 104–105 cm). **6, 8.** *Globigerinelloides* sp.; (6a–c) Sample 198-1209A-23H-3, 140–141 cm; (8a–c) Sample 198-1209A-23H-3, 100–101 cm. **7.** *Morozovella occlusa* (Sample 198-1209A-23H-3, 100–101 cm).

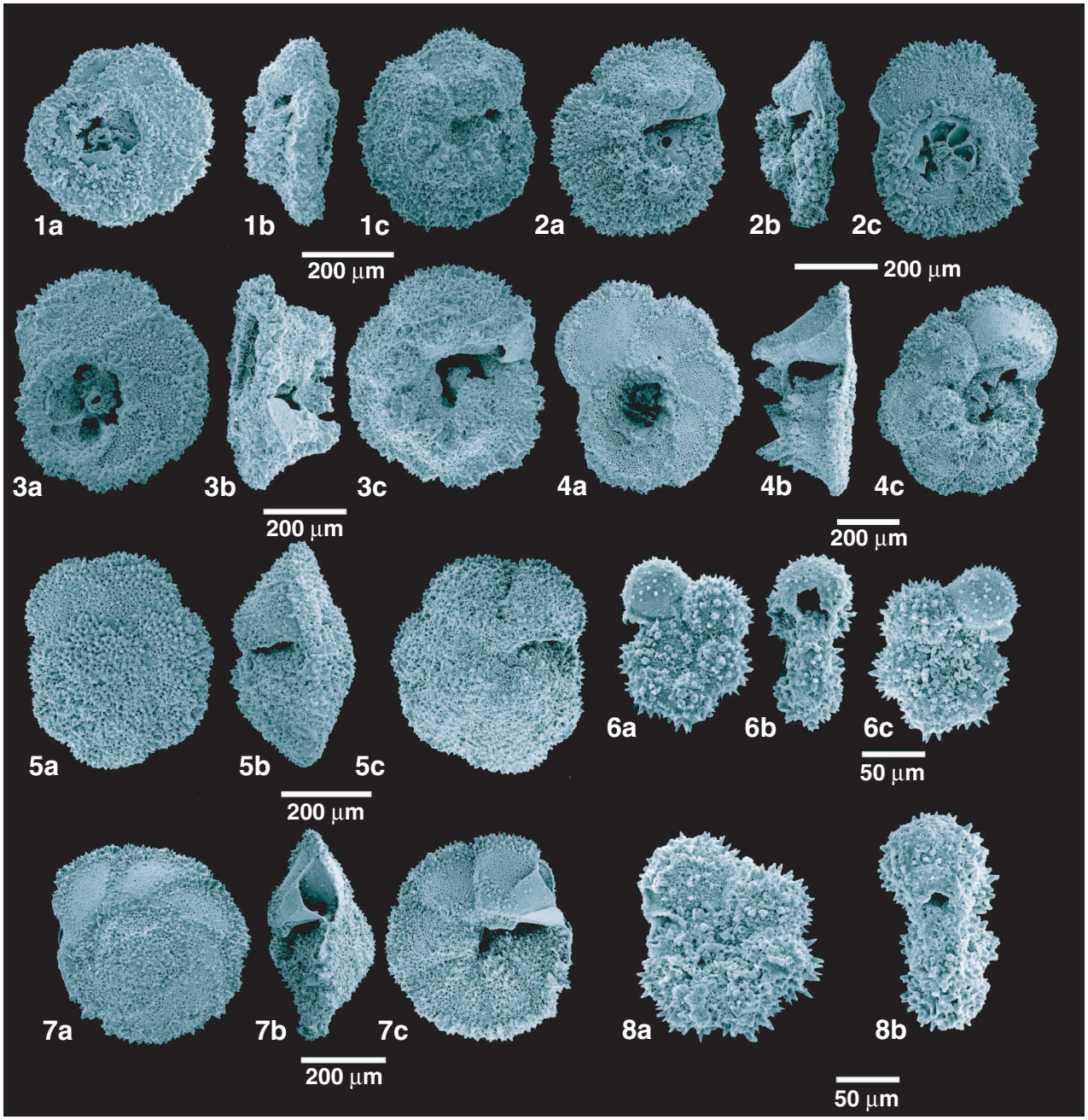

Plate P3. Scanning electron microscope pictures of washed residues selected from the three intervals: (1–4) above the clay-rich layer, (5–8) within, and (9–12) below **1, 2.** Sample 198-1209A-23H-3, 108–109 cm. **3, 4.** Sample 198-1211B-14H-4, 7–8 cm. **5, 6.** Sample 198-1209A-23H-3, 132–133 cm. **7.** Sample 198-1211B-14H-4, 32–33 cm. **8.** Sample 198-1210A-22H-3, 32–33 cm. **9, 12.** Sample 198-1212B-10H-5, 11–12 cm. **10, 11.** Sample 198-1209A-23H-4, 7–8 cm.

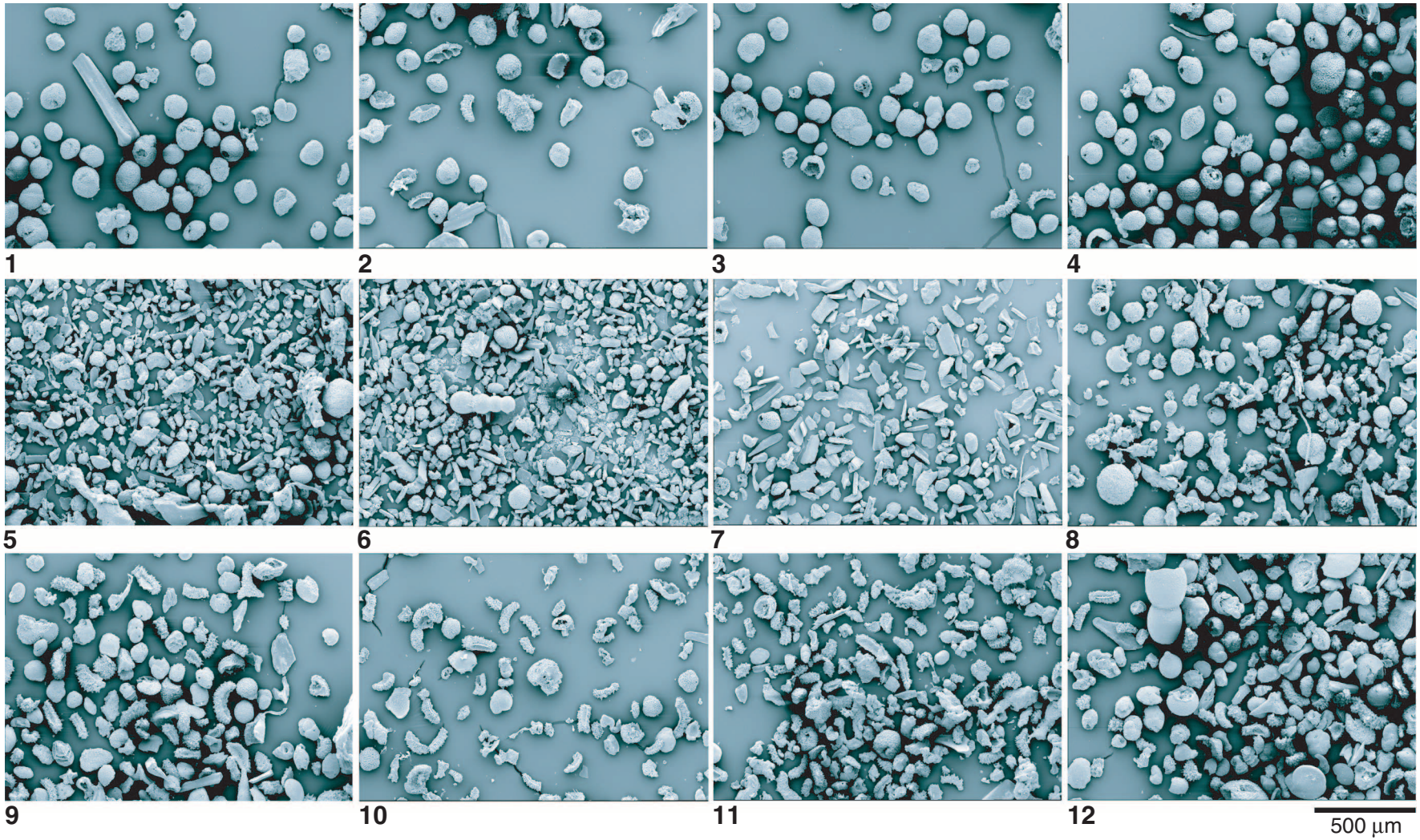

Plate P4. Scanning electron microscope pictures. **1, 5.** *Igorina tadjikistanensis;* (1a–c) Sample 198-1209A-23H-3, 127–128 cm; (5a–c) Sample 198-1209A-23H-3, 138–139 cm. **2, 8.** *Igorina albeari* "chubby;" (2a–c) Sample 198-1209A-23H-3, 118–119 cm; (8a–c) Sample 198-1209A-23H-3, 130–131 cm. **3, 10.** *Igorina albeari;* (3a–c) Sample 198-1209A-23H-3, 107–108 cm; (10a–c) Sample 198-1209A-23H-3, 114–115 cm. **4, 9.** *Igorina pusilla* "high trochospire;" (4a–c) Sample 198-1209A-23H-3, 127–128 cm; (9a–c) Sample 198-1209A-23H-3, 124–125 cm. **6, 7.** *Igorina pusilla* (Sample 198-1209A-23H-3, 127–128 cm).